Proceedings of the 9th International Symposium on Fluid-Structure Interactions, Flow-Sound Interactions, Flow-Induced Vibration & Noise
July 8-11, 2018, Toronto, Ontario, Canada

FIV2018-150

IN-PLANE FEI EVALUATION METHOD TAKING INTO ACCOUNT OF FRICTION DAMPING

Shingo Nishida
Mitsubishi Heavy Industries Ltd., Research and Innovation Center
Takasago, Hyogo, Japan

Seinosuke Azuma
Mitsubishi Heavy Industries Ltd., Research and Innovation Center
Takasago, Hyogo, Japan

Hideyuki Morita
Mitsubishi Heavy Industries Ltd., Research and Innovation Center
Takasago, Hyogo, Japan

Kazuo Hirota
Mitsubishi Heavy Industries Ltd., Research and Innovation Center
Takasago, Hyogo, Japan

Ryoichi Kawakami
Mitsubishi Heavy Industries Ltd., Nuclear Energy Systems Division
Kobe, Hyogo, Japan

Yoshihito Nishikawa
Kansai Electric Power Co., Inc.
Osaka, Osaka, Japan

ABSTRACT

Recently, tube-to-tube wear indications of triangular tube bundle steam generators (SGs) caused by in-plane fluid elastic instability (FEI) have been reported.

In the U-bend region of SGs with flat bar type supports, friction damping plays dominant role because U-bend tubes are supported only by friction forces in the in-plane direction. In the conventional way, friction force was evaluated as energy dissipation against external forced excitation. However, in the case of self-excited vibration like SG U-bend tubes, friction damped system shows the characteristics of forced self-excited vibration system intrinsically. Therefore, stability analyses using nonlinear friction forces and unstable fluid forces are required. We developed an evaluation method about this kind of friction damping. Nonlinear numerical simulation was conducted by taking into consideration of friction forces and unstable fluid forces. Furthermore, we conducted a validation test using single tube excitation test facility. The analytical results showed good agreement with the test results. The calculation procedure of friction damping used for FEI evaluation was verified.

NOMENCLATURE

W: Energy dissipation per 1 cycle, μ: Coefficient of friction
N: Normal contact force, x: Displacement
c: Viscous damping coefficient ρ: Fluid (averaged) density
c_{eq}: Equivalent damping coefficient U: Flow velocity
ζ_f: Equivalent friction damping, ω: Natural frequency(rad/s)
A: Vibration amplitude in Sinha's model
ζ_+: Added negative damping in Sinha's model
ε: Stiffness ratio in Sinha's model
f_0: External (Harmonic) force amplitude in Sinha's model
θ: Phase relationship in Sinha's model
Φ_{CPSD}: Cross power spectrum density, D: Tube diameter,
p,q: Node number of calculation model, f: Frequency (Hz)
L: Element length of FE model, C_f: Element correction factor
I: Correlation term, λ: Correlation length
z_1,z_2: Position for correlation calculation
y_1,y_2: Position from element end
k: Structural stiffness of simplified model
k_t: Tangential stiffness, τ: Time delay, G: Feedback gain,
m: Mass, F: Excitation force, k_{12}: Coupling stiffness

1 INTRODUCTION

Recently, it have been strongly recognized that triangular tube bundle have a potential to cause in-plane (flow direction) fluid elastic instability (FEI). Therefore, designers must pay attention to prevent in-plane FEI for U-bend tube bundle steam generators with flat bar type U-bend supports (e.g. Anti-Vibration Bars (AVBs)). For the out-of-plane direction, FEI motion is constrained by contact force even if small gaps exist between tubes and AVBs because AVBs are installed between columns of each tube row. For the in-plane direction, however, sufficient preloads at AVB contact positions and resulted friction constraints are required to prevent in-plane motion because tubes have no geometrical constraint for in-plane direction. Furthermore, friction damping effect plays dominant role to determine in-plane tube behavior if preloads were not sufficient. Although it is obvious that all contact positions had better to retain sufficient contact forces to prevent tubes from slipping in the in-plane direction, some unsupported points should exist because of variation of support conditions. Therefore, evaluation of friction damping is important for understanding in-plane FEI in actual SGs. In earlier studies, friction damping is dealt as an equivalent damping against external excitation force (i.e. random excitation). However, friction behavior must be treated as nonlinear forced self-excited vibration system when energy balance between FEI and friction force is considered. Because friction damping is generated by slip motion, tube must have certain amplitude driven by self-excitation force. This is a kind of limit cycle oscillation (LCO). And LCO will get less able to keep its amplitude and cause divergent vibration when FEI exceeds a certain level. This means occurrence of instability against friction force. This viewpoint is found in the system preventing self-excited vibration using friction damping intentionally. Sinha et. al. investigated stability boundary of friction damper used for gas turbine blade [1]. Gas turbine blades are exposed to nozzle wake force (forced excitation) and fluid force result from blade flutter (self-excited instability). In the study, friction damped system of blade was treated as a nonlinear forced self-excited vibration. They discussed characteristics of LCO and showed that limit of retaining of LCO means stability boundary of the system. Although they used harmonic balance method to analyze friction damped system, similar way of thinking is applied to time historical numerical calculation in this study because SG tubes are exposed to not harmonic force but random excitation and have more complicated characteristics (many point of contact, participation of higher order vibration modes).

2 LCO EVALUATION AND FRICTION DAMPING

Friction damping is generated by energy dissipation. Equivalent friction damping of vibration system exposed to force excitation can be calculated by energy dissipation of equivalent linear viscous damping when system settled in steady vibration amplitude. If Coulomb friction is assumed, energy dissipation is expressed as follows [2].

$$W = \mu N x \tag{2.1}$$

Although these characteristics are different from linear viscous damping intrinsically, friction damping can be approximated by linear damping ratio by focusing on a resonance behavior of certain vibration mode and thinking about energy dissipation per cycle. In the case of that 1DOF spring-mass vibration system continues steady sinusoidal motion being subjected only to linear viscous damping force, energy dissipation per cycle is calculated as follows.

$$W = \int c\dot{x}dx = c\int \dot{x}^2 dt = c\omega^2 x_0^2 F \int_0^{2\pi/\omega} \sin^2(\omega t - \varphi)dt = \pi c \omega x_0^2 \tag{2.2}$$

On the other hand, energy dissipation per cycle generated by friction force is $4\mu N x$ from equation 2.1. Substituting this into equation 2.2, equivalent friction damping is expressed as follows.

$$c_{eq} = \frac{4\mu N}{\pi \omega x_0}, \quad \zeta_f = \frac{\mu}{2\pi^3}\left[\frac{N}{M x_0 f^2}\right] \tag{2.3}$$

In existing study, various theoretical, experimental, semi-experimental evaluation method have been proposed [3]. And transfer function curve fitting method assuming 1DOF vibration system is often applied to experimental data and numerical simulation data. However, all these evaluation is based on the similar idea to equation 2.1 through 2.3 essentially.

Schematic illustration of energy balance between friction force and external excitation force against vibration amplitude is shown in Figure2.1. Resonant condition is assumed and perturbation of amplitude is discussed in the explanation below. In the case of viscous damped system, work by excitation force is linear proportional to amplitude, energy dissipation by viscous damping is proportional to the square of amplitude. These relationships make stable equilibrium point and this determine amplitude of the system. In the case of friction damped system, energy dissipation by friction damping is linear proportional to amplitude. If friction damped system has stable equilibrium point, energy input curve by excitation force is concave up because of its phase relationship under resonant condition. Equivalent damping is evaluated by assuming both system have the same damping ratio at the equilibrium point. There is no consideration of instability force in this model.

On the other hand, energy balances between friction force and external force and instability force. Shinha et. al. showed equilibrium condition of these three energy balance as follows.

$$A = \{4/\pi - f_0 \pm [(4/\pi - f_0)^2 - 32\zeta_+\omega/(\varepsilon\pi)]^{1/2}\}/\{4\zeta_+\omega/\varepsilon\}$$

$$\omega^2 = 1 - \varepsilon(\pi - \theta + 1/2\sin 2\theta)/\pi \tag{2.4}$$

Calculation example is shown in Figure 2.2. This equation has two steady amplitude solutions. Smaller one is stable equilibrium point, that is, LCO steady amplitude. Larger one is unstable saddle equilibrium point, that is, allowable upper limit of disturbance to be settled in LCO. If negative damping added by instability force (in this case, blade flutter) exceeds certain value, equation 2.4 has no solution, that is, there is no equilibrium point. This means system causes divergent vibration regardless of initial condition and disturbance. This situation must be defined "unstable" for friction damped forced self-excited vibration system. Schematic illustration of energy balance is shown in Figure2.3. When the instability level is small, system has stable equilibrium point. However, in the large instability case, system has no equilibrium point because increase rate of energy input become greater than that of energy dissipation in all amplitude range. Although this simple evaluation is for the system subjected to sinusoidal excitation, similar assumption can be applied to SG tube that has random response nature.

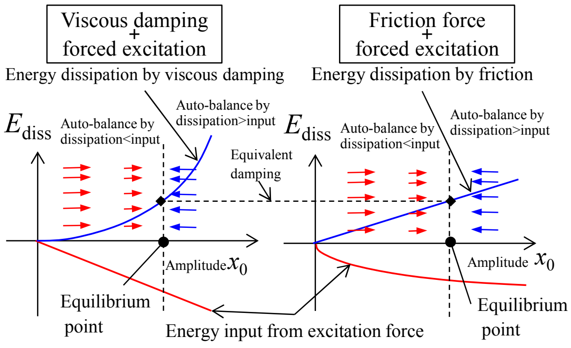

FIGURE 2.1: Energy balance of friction damped system

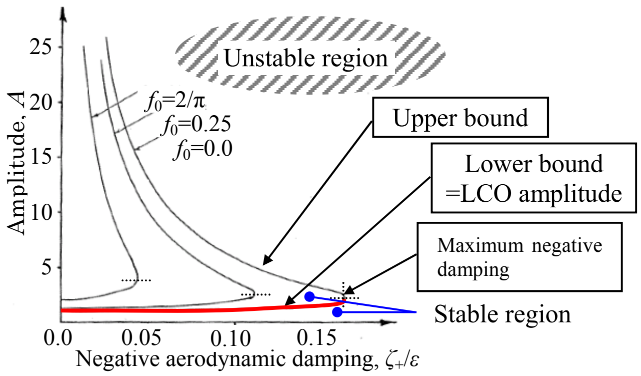

FIGURE 2.2: Calculation result of equation 2.4

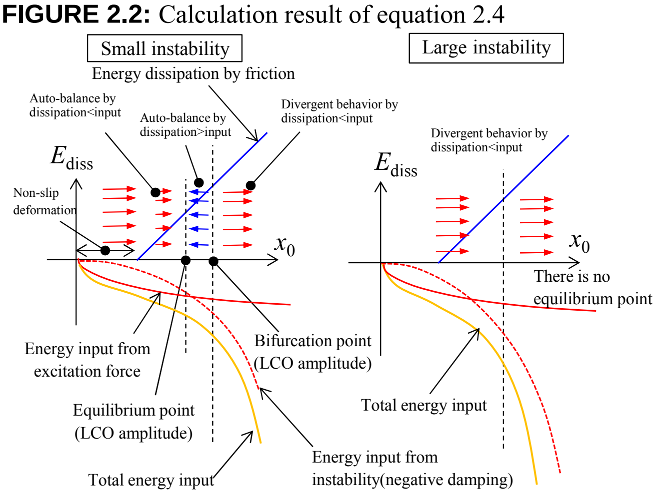

FIGURE 2.3: Energy balance of friction damped LCO

3 CALCULATION MODEL

3.1 Structural model and random excitation force

FEM model consist of beam element is used for time historical calculation of tube motion. Modal superposition method is applied and contact force is evaluated as external force of physical coordinate at contact positions. Spatial correlated fluid random force is applied to U-bend region for both out-of-plane and in-plane direction. Excitation forces for out-of-plane direction generate contact force and resulted friction force at gap condition AVB position. Excitation force for in-plane direction acts as forced external force in the model of equation 2.4.

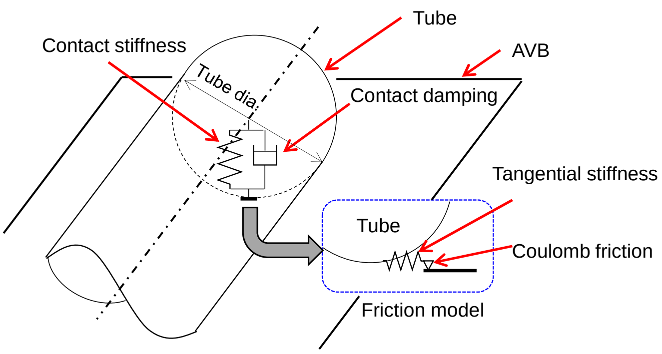

FIGURE 3.1: Contact and friction force model

3.2 Contact and friction model

Contact is modeled by gapped linear spring and damper. Friction is modeled by Coulomb friction with tangential spring. Tangential spring is representation of local tangential deformation at contact points. Schematic of models are shown in Figure 3.1.

3.3 Instability force model

Although various fluid force model is available, linear negative damping is applied for simplicity. Negative damping was calculated by applying negative modal damping ratio to target in-plane vibration mode.

4 CALCULATION RESULT AND VALIDATION TEST

4.1 Calculation of SG tube response

All of numerical calculations in this study were conducted by MHI proprietary code "IVHET2". Time history numerical calculations were conducted for the model of SG tube geometry. Random excitation force, added negative damping ratio by fluid elastic instability, drag static force and contact condition at AVBs were taken into consideration. Schematic of analytical model is shown in Figure 4.1. Random excitation force is calculated as follows [4].

$$\Phi_{CPSD}(p,q) = 7.5\times\left(\frac{\rho U^2 D}{2}\right)^2\left(\frac{D}{U}\right)\times 5\times 10^{-5}\left(\frac{fD}{U}\right)^{-2.7}\times I(p,q)\times\left(\frac{U_p U_q}{U^2}\right)^2\left(\frac{\rho_p \rho_q}{\rho^2}\right)$$

$$I(p,q) = e^{-\frac{|Z_p - Z_q|}{\lambda_C}},\ C_f = \frac{1}{L_p L_q}\int_{E_p}\int_{E_q} e^{-\frac{|y_2 - y_1|}{\lambda_C}}\, dy_1 dy_2 \qquad (4.1)$$

Used random excitation force PSD model and applied flow condition is shown in Figure 4.2. Although it was excessively conservative for actual situation, all AVB contact positions were modeled as gapped (with no preload) condition. Model specifications are shown in Table 4.1. Calculation is conducted in two gap size as shown in Table 4.2. Calculation conditions are shown in Table 4.3. Linear negative modal damping ratio is applied to in-plane first vibration mode in the time history numerical simulation. Negative damping revel was gradually increased and occurrence of instability was judged by sudden increase of in-plane vibration amplitude.

Calculation result is shown in Figure 4.3. Tube response displacement RMS showed sudden increase with -13% added damping for 0.2mm gap condition and with -22% added damping for 0mm gap condition. This means they can endure negative damping up to -12%, -21% respectively, that is, these values are friction damping effect against instability force. Response amplitude showed similar trend to lower bound of Figure 2.2. If the friction damping is calculated by curve fitting method from response displacement spectrum with no negative damping, equivalent damping ratio is 25% for 0.2mm gap condition. It was impossible to calculate by the same way for 0mm gap condition because resonance peak was unclear by heavy damping effect. This result means friction damping calculated by curve fitting of equivalent 1 DOF system could be unsafe evaluation for small amplitude conditions.

Narrow gap condition showed higher stability limit. This is thought to result from greater energy dissipation by longer cumulative contact time of narrow gap. This indicates that gap size control could be design criteria for prevention of in-plane FEI.

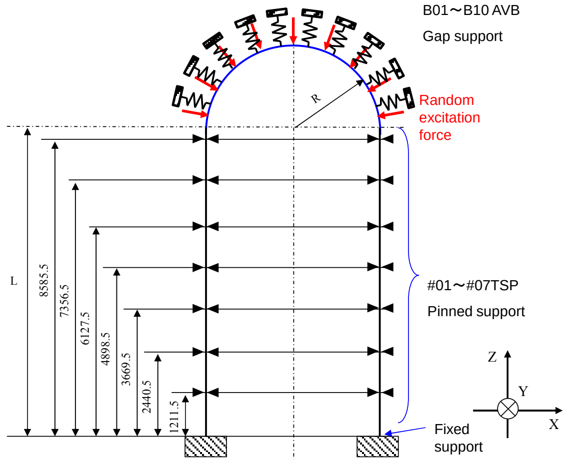

FIGURE 4.1: Analytical model for SG tube

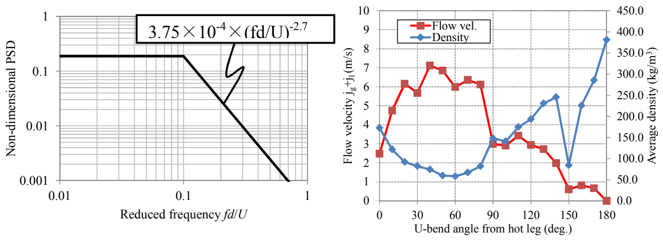

(a) Non-dimensional PSD (b) Flow vel. density distribution

FIGURE 4.2: Random excitation PSD and flow condition

TABLE 4.1: Model specifications

Tube dia.	19.05mm	**Radius of U-tube**	1689.1mm
Tube wall thickness	1.09mm	**Number of AVB contact point**	10 (All gapped)
P/D	1.33 (Triangular array)	**Length of straight tube**	8985.7mm
Contact stiffness	6900 N/mm	**Tangential stiffness**	7500 N/mm
Contact damping	200 Ns/m	**Coefficient of friction**	0.4
Material	TT690		

TABLE 4.2: Calculation case

	Case1	**Case2**
AVB contact condition	Gap condition at all AVBs	Gap condition at all AVBs
Gap size	0mm	0.2mm (diametric gap)

TABLE 4.3: Calculation condition

Duration	25s	**Considered vibration mode**	All modes less than 1000Hz
Output step	0.1ms	**Damping ratio**	1.6% for up to 100Hz 10% for others
Solver	Dormand-Prince	**Time step**	Variable (smaller than 0.1ms)

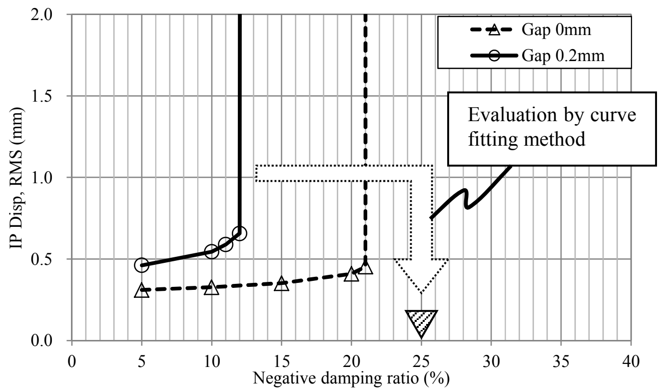

FIGURE 4.3: Calculation result of SG tube response

4.2 Validation test and calculation result

Validation test was conducted to investigate this instability mechanism. Setup of the test is shown in Figure 4.4. Specifications of test equipment are shown in Table4.4. All 12 AVBs were adjusted to 0.4mm diametric gap condition. Random excitation force was inputted by electro-magnetic exciter from both in-plane and out-of-plane direction. Velocity feedback system was applied for in-plane direction to simulate negative damping of instability force.

Numerical calculation was conducted using measured excitation force by same procedure shown in section 4.1. Calculation result is shown in Figure 4.5. Trend of in-plane tube response and occurrence point of instability agree well with test result.

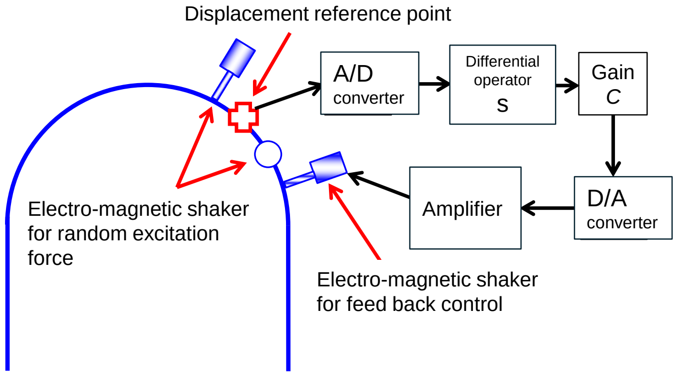

(a) Schematic of excitation system

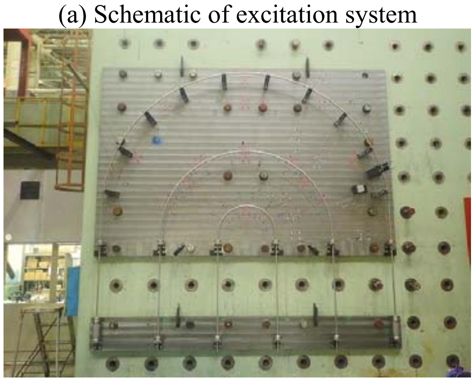

(b) U-tube used for excitation test

FIGURE 4.4: Validation test setup

TABLE 4.4: Specifications of test equipment

Tube dia.	19.05mm	**Radius of U-tube**	1689.1mm
Tube wall thickness	1.09mm	**Number of AVB contact point**	10
Contact stiffness	6500 N/mm	**Tangential stiffness**	7500 N/mm
Contact damping	110 Ns/m	**Coefficient of friction**	0.4
Material	TT690		

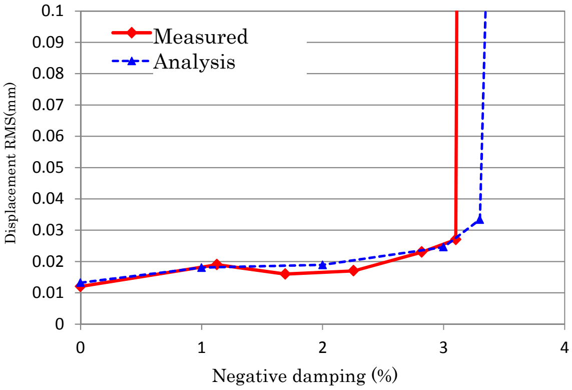

FIGURE 4.3: Calculation result of validation test

5 DISCUSSIONS

Although linear negative damping was applied in calculation above for simplicity, fluid elastic force as actual physical phenomenon is different at two points below.

(1)Linear negative damping was assumed in this study. However, fundamental mechanisms of unsteady fluid force contain time delay, amplitude dependence and other nonlinear effects. Commonly, unsteady fluid force is modeled as frequency-dependent linear added stiffness and damping. This assumption is thought to be reasonable under infinitesimal amplitude condition. However, it depends on condition whether this assumption is appropriate or not under finite amplitude condition like LCO.

(2)Although instability of single tube has been discussed in this study, in-plane FEI is caused by coupling effect of more than two tubes in general. For multiple degrees of freedom systems, nonlinear phase relationship between instability force and friction force act on each tubes could be different from 1DOF system. This will result in difference of stability boundary.

To investigate effect of these characteristic to stability boundary, simplified calculations were conducted as shown below. Simplified calculation model is shown in Figure 5.1. Instability behavior was investigated using 1DOF or 2DOF spring-mass vibration model subjected to random excitation force and Coulomb friction force and various instability force (Case1: linear negative damping, Case2: time delay, Case3: asymmetric stiffness coupling). Following parameters were set to the same for all cases; steady friction force μN, tangential stiffness k_t, mass m and structural stiffness k. Random excitation force that has the same PSD as used in section 4.1 was used and non-correlated random force was applied to each mass for 2DOF calculation case. Instability revel (scaled in equivalent negative damping value) was gradually increased and occurrence of instability was judged by sudden increase of in-plane vibration amplitude RMS. Calculation cases are shown in Table 5.1. Specifications of calculation cases are shown in Table 5.2. Calculation results are shown in Figure5.2.

Response displacement RMS showed similar trend as calculation result of Chap.4. From comparison between Case1 and Case2, following characteristics were found. Basically, calculation result of linear negative damping and time delay showed similar trend of RMS increment. For small random excitation force, critical damping is almost the same between both cases. However, some difference was found for large excitation level cases. This is result from violation of infinitesimal amplitude assumption, that is, it is difficult to assume time delay as linear damping in high excitation level, large amplitude condition. From comparison between Case1 and Case3, following characteristics were found. Trend of response displacement RMS is fundamentally different between both cases. And critical damping ratio also definitely different regardless of its random excitation level. This result from because phase relationship between friction force and instability force in 2DOF stiffness coupled model is intrinsically different from that of 1DOF model, energy dissipation thought to be different. Considering SG tube condition, contact condition and number of participated tube are more complicated. Therefore, appropriate assumption of instability intensity of reduced DOF model remains challenging problem.

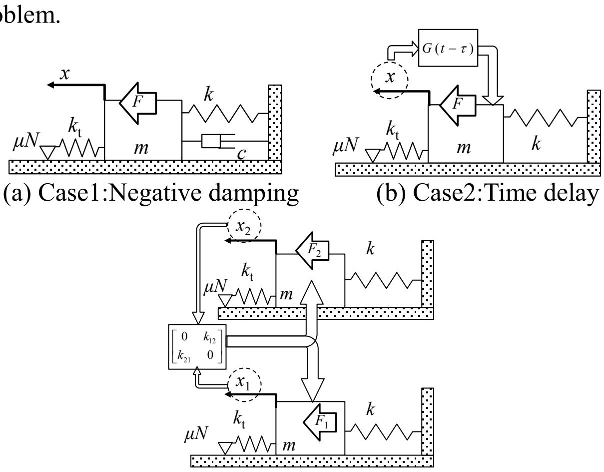

(a) Case1:Negative damping (b) Case2:Time delay

(c) Case3:Coupling stiffness

FIGURE 5.1: Simplified calculation model

TABLE 5.1: Calculation cases

Cal. case	DOF	Instability type	Forced excitation	Excitation level	Eq. damp.
Case1	1	Negative damping	1 Random wave	0.05Nrms through 0.53Nrms	0 through -20%
Case2	1	Time delay			
Case3	2	Stiffness coupling	2 Random waves		

TABLE 5.2: Specifications of calculation cases

Cal. case	Structural parameter	Instability intensity
Case1	Mass= 1kg	0 through -26.5 Ns/m
Case2	Stiffness= 4.3×10^3N/m	Time delay: τ=0.01s (Fixed) Gain: G=0 through 2.6×10^3 N/m
Case3	Friction force μ=0.5,N=0.5N	Coupling stiffness k_{12}=0 through 1.75×10^3 N/m, k_{21}=-k_{12}

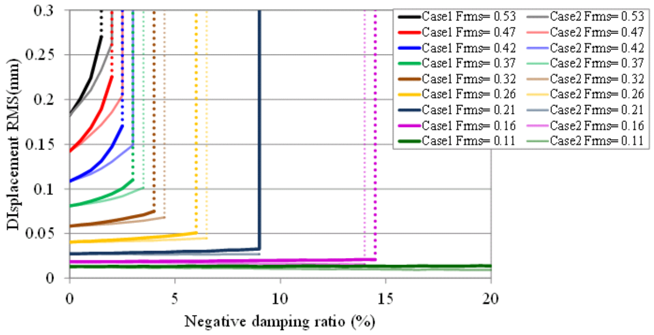

(a) Comparison betwee Case1 and Case2

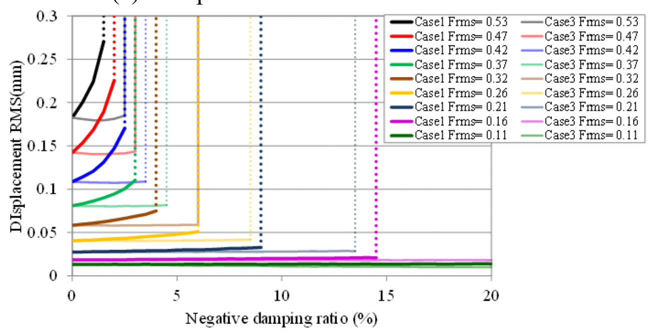

(b) Comparison betwee Case1 and Case3

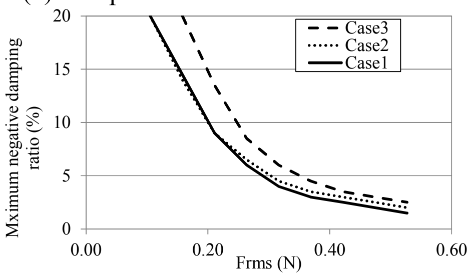

(c) Excitation level vs maximum damping

FIGURE 5.2: Calculation result of simplified calculation

6 CONCLUSIONS

Numerical simulations were conducted for judgment of stability of SG tube subjected to random excitation force, fluid elastic instability and friction force based on the concept of forced self-excited vibration. Similar way of thinking to friction damped gas turbine blade flutter was introduced to SG tube in-plane instability. Following conclusion was derived from evaluation of SG tube and comparison between measurement and calculation.

(1) Characteristics of in-plane instability subjected to friction and random excitation is different from equivalent friction damping ratio of forced excitation intrinsically. Stability judgment can be conducted by numerical simulation taking into account of contact, friction, random excitation and fluid elastic instability.

(2) Stability analysis for SG tube design can be conducted by applying contact/gap condition to tube calculation model and expected added negative damping derived from flow condition. Basic calculation procedure was confirmed by validation test. However, reasonable assumptions of contact/gap condition for actual SGs and statistical approach remains challenging problems.

(3) Gap size control could be design criteria for prevention of in-plane fluid elastic instability with friction force even if gap condition is assumed at all AVB contact points.

(4) Although stabilize effect by friction force depends on characteristics of stability force, it can be simulated by numerical calculation. However, precise assumption of instability force is thought to be challenging because energy dissipation effect of friction force against instability force depends on number of participated tube if more than two tubes are subjected to friction force.

(5) In the case of small vibration amplitude, friction damping calculated by the assumption of equivalent viscous damping could be larger value than endurance limit of negative damping against friction-damped forced self-excited vibration system. This means FEI evaluation by Conners equation could be unsafe evaluation if the former friction damping were used.

ACKNOWLEDGMENTS

This experimental work has been carried out as a Japanese government-subsidized R&D project, “The Safety Improvement of Nuclear Facilities” with the participation of The Kansai Electric Power Co., Inc., Kyushu Electric Power Co., Inc., The Japan Atomic Power, The Institute of Applied Energy, And Mitsubishi Heavy Industries, LTD.

REFERENCES

[1] A. Shinha, J. H. Griffin, 1983. “Friction Damping of Flutter in Gas Turbine Engine Airfoils”. *Journal of Aircraft*, Vol. **20**, No. 4, pp. 372–376.
[2] J.P. den Hartog, 1956 Mechanical vibrations, DOVER
[3] M.J. Pettigrew, 2011, Damping of Heat Exchanger Tubes in Liquids: Review and Design Guidelines, *Journal of Pressure Vessel Technology*, Vol. **113**, pp. 014002-1–11.
[4] EPRI, Steam Generator Vibration and Wear Prediction, TR-103502